Journal of Power Sources 196 (2011) 8728–8734

Contents lists available at ScienceDirect

Journal of Power Sources

journal homepage: www.elsevier.com/locate/jpowsour

Mechanical behavior of a battery separator in electrolyte solutions

Azadeh Sheidaei[a], Xinran Xiao[a,*], Xiaosong Huang[b], Jonathon Hitt[c]

[a] Department of Mechanical Engineering, Michigan State University, 2727 Alliance Dr, Lansing, MI 48910, USA
[b] Chemical Sciences & Materials Systems Lab, General Motors Global R&D, 30500 Mound Rd, Warren, MI 48090, USA
[c] Optimal Inc, 14492 Sheldon Rd, Suite 300, Plymouth Twp, MI 48170, USA

ARTICLE INFO

Article history:
Received 24 May 2011
Accepted 6 June 2011
Available online 12 June 2011

Keywords:
Battery separator
Li-ion batteries
Mechanical property
Polypropylene

ABSTRACT

The structural integrity of the separator is crucial to the abuse tolerance of a battery. To estimate its stress level in a battery, the mechanical property of the separator in situ in the battery environment must be known. This work investigated the tensile behavior of a single layer polypropylene (PP) separator in electrolyte solutions for Li-ion batteries using a dynamic mechanical analyzer (DMA). The measurements were carried out in both dry (ambient) and wet conditions for both the machine direction (MD) and the transverse direction (TD). In the wet condition, samples were submerged either in a DMC solvent or in a electrolyte solution of 1.1 M LiPF6 in EC/DMC (1/1 by volume). The DMA experiments were performed under uniaxial tension, creep, and frequency sweep modes. The results in all three modes demonstrated that the mechanical properties of the separator were significantly lower in wet conditions. For instance, in the MD, relative to the dry condition, the ratio of the Young's modulus was about 0.49 and 0.52 for DMC and 1.1 M LiPF6 in EC/DMC, respectively. The results indicate that the mechanical properties measured in dry condition using samples that had been preconditioned in solutions are not sufficient to represent the in situ material behavior.

1. Introduction

Improving the performance of the separator beyond the status-quo remains one of the primary challenges for large-scale Li-ion batteries used in high energy applications. A basic Li-ion battery cell consists of three components including the positive and negative electrodes sandwiching a separator, all of which are saturated with a liquid electrolyte. The separator, a porous membrane that prevents physical contact between the positive and negative electrodes, enables ionic transport between the electrodes [1–4]. Three common types of separators are polymeric membranes, nonwoven mats, and ceramic enhanced membranes. Currently, polymeric membranes are used predominantly due to their low cost and small relative thickness. A thin separator will facilitate the ionic transport and provide higher energy and power densities. However, polymeric separators must possess sufficient mechanical properties to withstand the stretching during cell assembly, cyclic deformation of the insertion electrodes, and resist penetration due to dendritic growth on the electrodes or from foreign debris introduced in the battery manufacturing process [4–9]. A short circuit due to separator failure may lead to a thermal event [10,11].

It is well recognized by the Li-ion battery community that stress can have a significant impact on the performance of the separator. Currently, there is no method to evaluate the stress inside a battery. Consequently, there are no clear guidelines for the mechanical property requirements for the separator yet. To improve the performance of battery separators, the stresses upon the separator in situ must be known. To evaluate the intercalation and thermal mismatch induced stresses in the separator, multi-scale multi-physics models are currently under development [12–14]. Measuring the mechanical properties of a separator in situ in a battery is one of the tasks in this effort.

The mechanical properties of a separator may be measured following the American Society for Testing and Materials (ASTM) standards. The tensile property is commonly measured per ASTM D-638 and tear resistance per ASTM D-1004 [1]. Load frames [15–18] and dynamic mechanical analyzers (DMA) [3,19,20] have been employed to investigate the mechanical properties of polymeric separators. Love [20] investigated the behavior of four types of separators in both as received condition and after being exposed to various immersion environments and reported small changes in mechanical properties. A common belief is that electrolyte solutions have little effect on separators. To verify this, experiments in situ in electrolytes are required.

In this work, the tensile behavior of a commercially available polypropylene separator was investigated both in a dry condition

* Corresponding author. Tel.: +1 517 884 1606; fax: +1 517 884 1601.
E-mail addresses: Xinran@egr.msu.edu, xinran@msu.edu (X. Xiao).

0378-7753/$ – see front matter © 2011 Elsevier B.V. All rights reserved.
doi:10.1016/j.jpowsour.2011.06.026

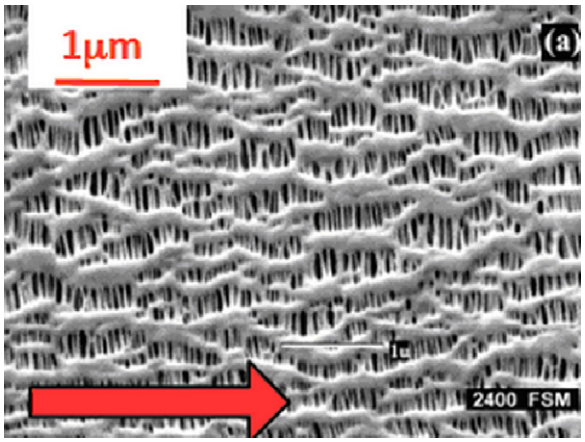

Fig. 1. Scanning electron microscope (SEM) image of the surface of a single layer polypropylene separator [1]. The MD is perpendicular to the arrow, which indicates the TD.

and in electrolyte solutions using a DMA. Static, creep and frequency sweep experiments were conducted.

2. Experimental

A commercially available separator, Celgard 2400, was investigated in this work. Celgard 2400 is a single layer microporous polypropylene (PP) membrane. The micropores are introduced through a dry process, in which the membrane is subjected to a uniaxial stretching. This process leads to a non isotropic microstructure, as shown in Fig. 1 [1], giving the membrane two distinct material directions which are commonly referred to as machine direction (MD) and transverse direction (TD).

All mechanical testing were carried out under a tensile mode using a DMA with a submersion film/fiber clamp [21]. The tensile clamp supplied by TA Instruments has a fixed gauge length of 15 mm. The samples, in the form of long strips with a nominal width of 6 mm, were cut using a razor blade. The sample width was then measured, on a flat surface, using a Vernier caliper. The separator has a nominal thickness of 25 μm, which gives a nominal sample cross section area 6 mm × 0.025 mm.

Sample preparation is one of the most important factors in achieving accurate and reproducible measurements. Fig. 2, from left to right, shows the cutting process and sample assembly in the submersion film/fiber clamp. For samples in the TD, extra care was taken by cutting the samples, using a concave scalpel (single pass) and a straight edge (to guide the slice), between a folded sheet of lined paper (spaced at 6 mm).

The samples were tested in both dry and wet conditions. Two solutions were used in submersion tests. One is the dimethyl carbonate (DMC), a common solvent in electrolyte for lithium-ion batteries, and the other is 1.1 M LiPF6 in a mixed solution of ethylene carbonate (EC) and dimethyl carbonate (DMC) in 1:1 volume ratio (1.1 M LiPF6 in EC/DMC). Both DMC and EC/DMC evaporate in air and hence the bath needs to be refilled frequently and a fresh solution was used each day.

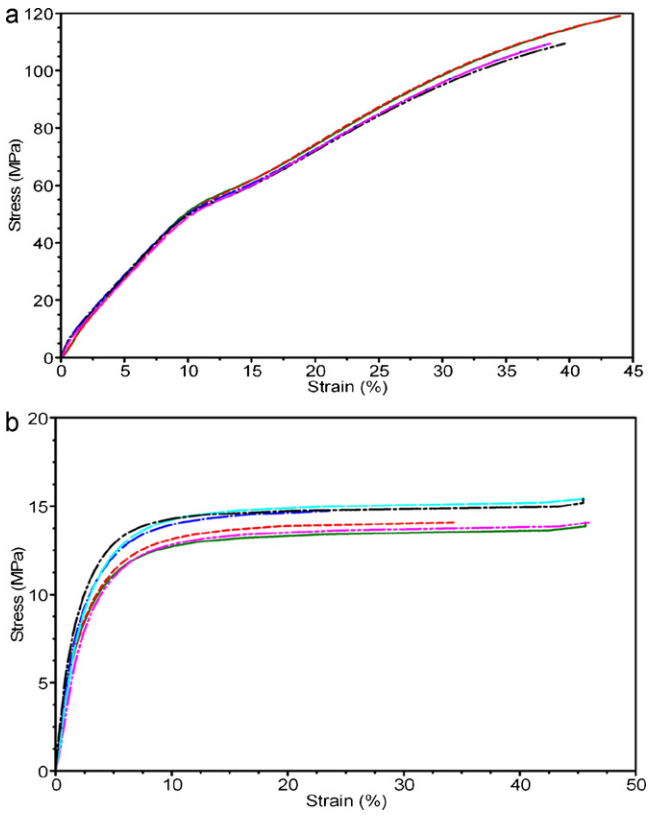

Fig. 3. Stress versus strain curves for the separator in the dry condition (a) MD and (b) TD.

In the dry condition, the samples were tested as received and after having been immersed in solutions. In the wet condition, the sample was left in the solution for 20 min to reach saturation before testing began. The time period of 20 min was established after a series of "sample pre-testing retention time" experiments were performed. It was observed that a longer immersion even up to a week, did not affect the results.

To examine the repeatability of the results, the measurements were carried out at two laboratories. TA Instruments 2980 DMA was used at both locations. All experiments used a preload of 0.01 N. All results reported in this paper were obtained at room temperature. The ambient temperature varied between 22 and 28 °C.

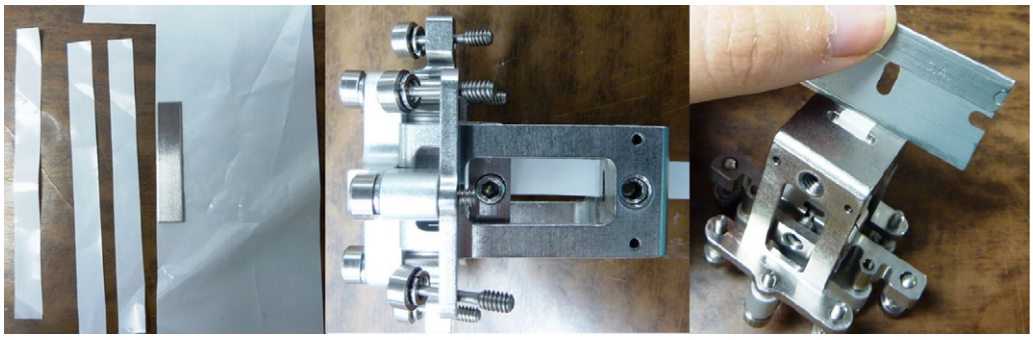

Fig. 2. Sample preparation and installation.

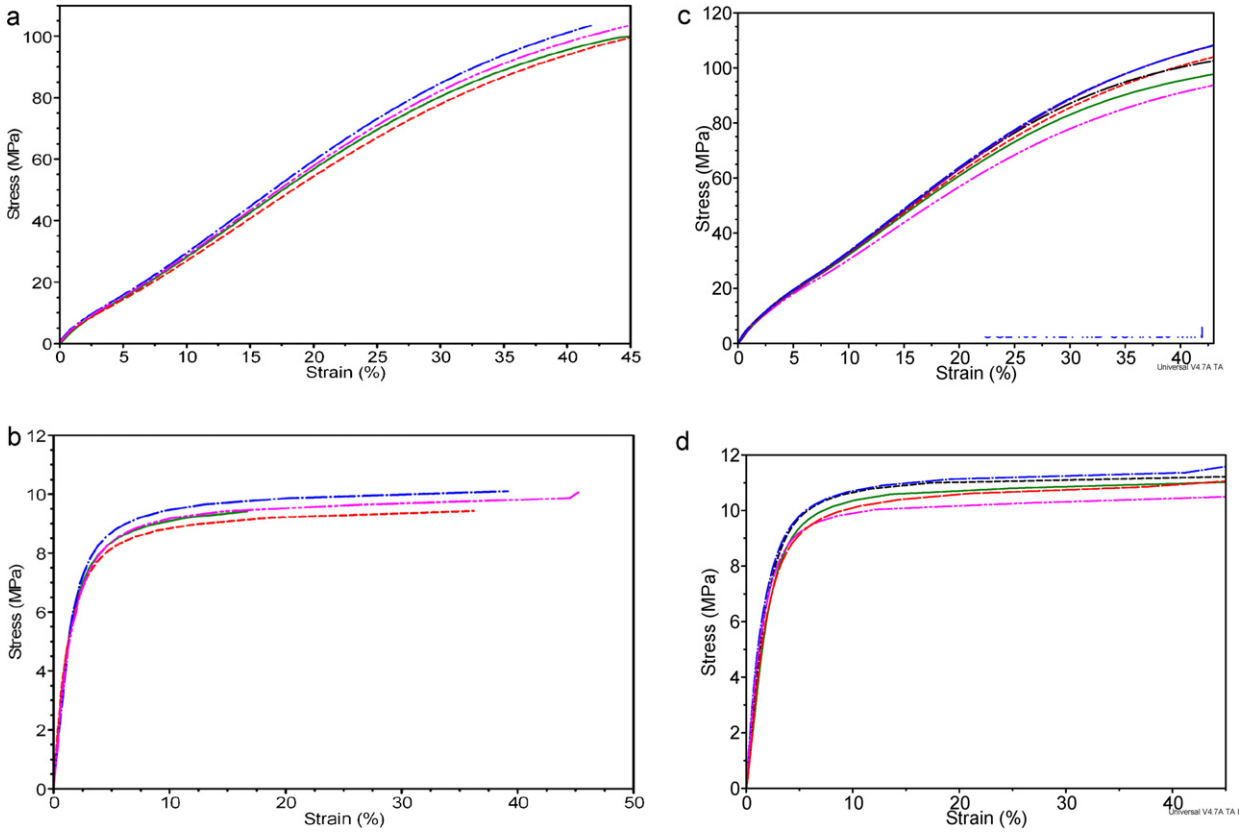

Fig. 4. Stress versus strain curves for the separator under submersed conditions. (a) MD in DMC; (b) TD in DMC; (c) MD in 1.1 M LiPF6 in EC/DMC; and (d) TD in 1.1 M in LiPF6 in EC/DMC.

3. Results and discussion

3.1. Tensile behavior

The uniaxial tensile stress–strain behavior was investigated under a force controlled mode with a loading rate of 1 N min^{-1} (6.66 MPa min^{-1}) at the room temperature. The tensile tests were carried out in both MD and TD. Limited by the maximum stroke of the DMA, the samples can only be tested up to about 45% of strain and the samples were not ruptured when tested in MD. Some TD samples ruptured at strain levels above 20%.

Fig. 3a and b presents the tensile engineering strain–stress curves in the MD and TD in the dry condition, respectively. The engineering stress is defined as [22]

$$\sigma = \frac{F}{A} \tag{1}$$

where F is the load and A is the original cross sectional area of the sample. The engineering strain is defined as [22]

$$\varepsilon = \frac{\Delta l}{l_0} \tag{2}$$

where l_0 is the original gauge length, Δl is the elongation measured over the gauge length. In this work, a fixed distance of 15 mm between the clamps was taken as the gauge length. The displacement of the moving clamp, recorded by the DMA, was taken as the elongation.

As shown, the stress–strain curves in MD and TD differ significantly. The MD stress–strain curves displayed a nearly linear region below 10% of strain, a softening region between 11 and 15% of strain, and then a slightly stiffer region at higher strains. This forms a knee in the stress–strain curve. The TD stress–strain curves displayed a nearly perfect plastic flow behavior and a clear yield point, giving an average yield strength of about 14.2 MPa.

Fig. 4a and b presents the stress–strain curves measured on samples submersed in DMC in MD and TD, respectively. The shape of the curves beard some likeness of that measured in dry condition responses but the response was significantly softer. The MD curves exhibited a mild softening and hardening transition but did not have a clear knee shape as that in the dry condition. The TD curves exhibited a perfect plastic flow behavior similar to that in the dry condition but the averaged yield strength was reduced to 9.6 MPa. The experiments were also carried out in 1.1 M LiPF6 in EC/DMC

Table 1
Tensile properties of the separators.

	Measured modulus (MPa)	Yield stress (MPa)	% strain that non-linearity occurred
Dry, MD	843 ± 20	–	0.87
Dry, TD	430 ± 23	14.2 ± 0.4	0.64
Submersed in DMC, MD (ratio to dry)	409 ± 28 (0.485)	–	0.65 (0.747)
Submersed in DMC, TD (ratio to dry)	377 ± 10 (0.877)	9.6 ± 0.2 (0.677)	0.45 (0.703)
Submersed in 1.1 M LiPF6 EC/DMC, MD (ratio to dry)	437 ± 15 0.518	–	0.65 (0.747)
Submersed in 1.1 M LiPF6 EC/DMC, TD (ratio to dry)	388 ± 42 (0.903)	10.8 ± 0.4 (0.762)	0.77 (1.2)

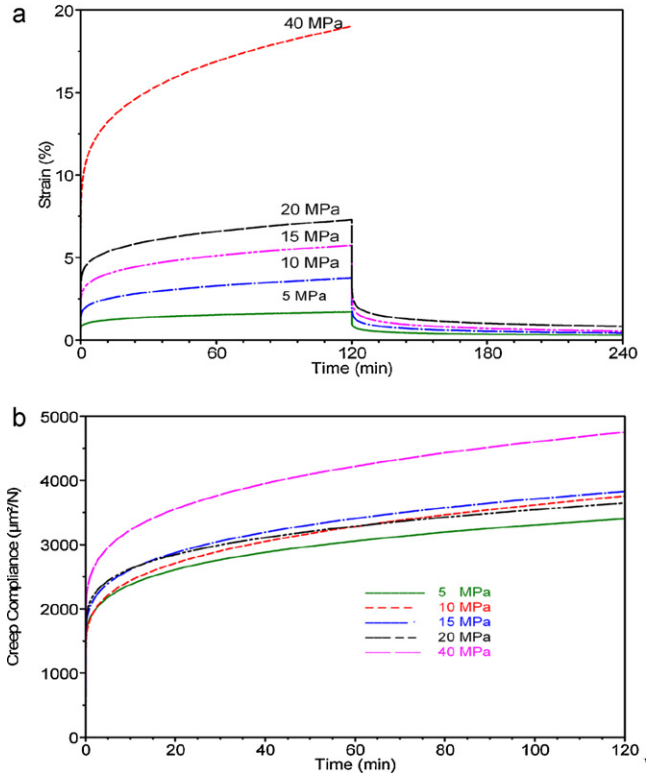

Fig. 5. (a) Creep and recovery strains and (b) creep compliances measured in the dry condition.

(Fig. 4c and d), and the behaviors were similar to those tested in DMC.

Table 1 provides a summary of the tensile mechanical properties. The Young's modulus was determined by fitting the linear portion of the stress–strain curves in the strain range of 0–0.4%. When being soaked in DMC, the modulus was found to decrease to 48.5% in the MD and 87.7% in the TD, and the yield strength in the TD was reduced to 74.7% in terms of ratio to that of measured in the dry condition. The properties measured in the electrolyte were slightly higher than that in DMC, but were in the range of experimental error. The ratio of the modulus to the dry condition was 51.8% in the MD and 90.3% in the TD.

3.2. Creep response and linear viscoelastic model

3.2.1. Creep response

A series of creep tests were performed with samples in the MD at distinct loads for both dry and wet conditions. A new sample was used in each creep test. For the dry condition, the samples were subjected to a constant load for 120 min. After the load was removed, the samples were left in the clamp for another 120 min and their recovery responses were recorded. For the wet condition, to reduce the effect of solvent evaporation, the creep and recovery periods were reduced to 60 min.

Fig. 5a depicts the creep responses measured in the dry condition for the MD at 5, 10, 15, 20, and 40 MPa. Creep recovery was not performed for 40 MPa stress level. The creep behaviors at the four lower stress levels appear to be in the range of linear viscoelasticity, proven by the nearly load proportional spacing between the curves. A linear viscoelastic material would exhibit a creep strain proportional to the stress level, and the creep compliance, $J = \varepsilon(t)/\sigma$, would be independent of the stress level. Fig. 5b presents the creep compliance curves at five stress levels. As shown, the curves at four lower stress levels collapsed into one group, indicating that

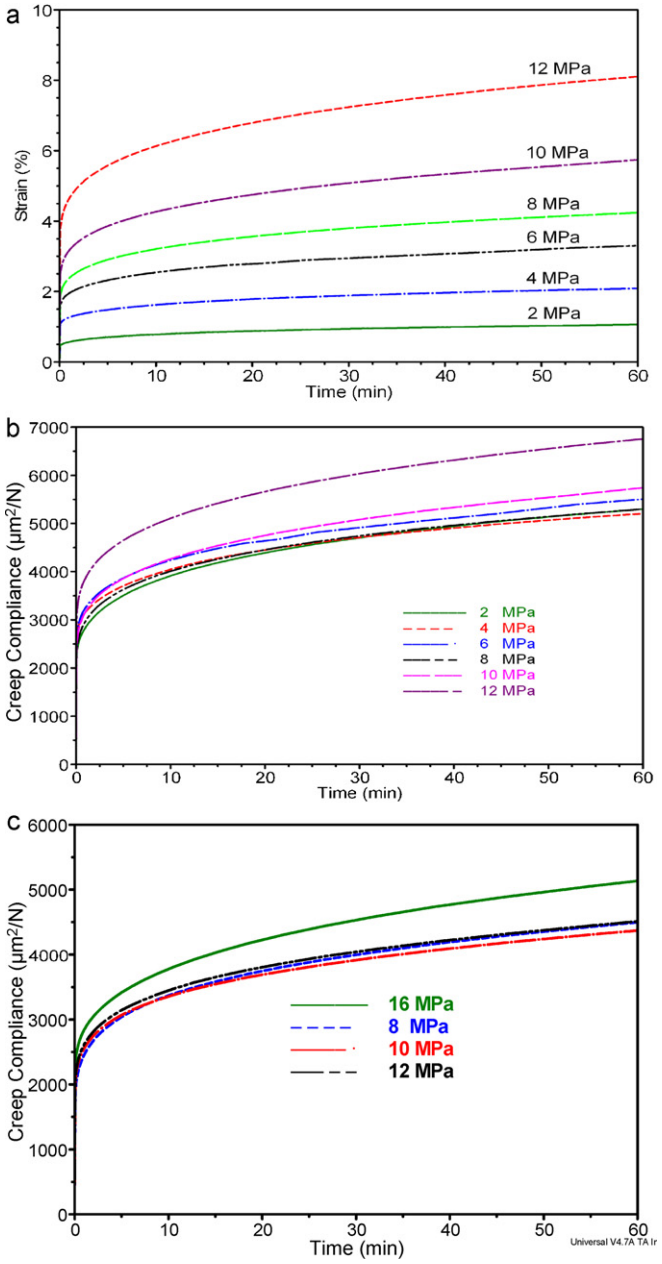

Fig. 6. (a) Creep and recovery strains measured in DMC, (b) creep compliances in DMC, and (c) creep compliances in 1.1 M LiPF6 in EC/DMC.

the creep response is linear at least up to 20 MPa. The curve for 40 MPa was in a separate group, showing the effect of nonlinear viscoelasticity.

The creep tests were also performed on samples submersed in liquids at room temperature. Due to softening, creep tests were conducted at lower stress levels compared to those for dry samples. Starting from 2 MPa and incrementing by 2 MPa, creep tests for 6 stress levels up to 12 MPa were conducted in the MD. Fig. 6a and b presents the creep strains and creep compliances measured on samples in DMC. The creep response was linear up to 10 MPa. The creep compliance at 12 MPa was higher than those at other stress levels, indicating the tendency to nonlinearity. The trend of creep result for samples in 1.1 M LiPF6 in EC/DMC was similar to that in DMC but seemed to be slightly stiffer. Fig. 6c presents the creep compliance measured in 1.1 M LiPF6 EC/DMC. As shown, the linear elastic range was up to 12 MPa.

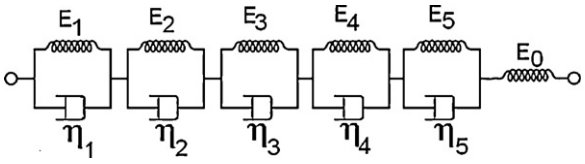

Fig. 7. Schematic of a Kelvin–Voigt model for a linear viscoelastic solid.

3.2.2. Viscoelastic model

The linear viscoelastic response of the separator was fitted by a model with five Kelvin–Voigt elements, as depicted in Fig. 7 [23]. The Kelvin–Voigt model can be described mathematically by a Prony series [22]

$$J(t) = J_0 + \sum_{i=1}^{5} J_i \left(1 - \exp\left(\frac{-t}{\tau_i}\right)\right) \quad (3)$$

where J_0 is the instantaneous compliance, J_i is the creep constant and τ_i is the retardation times associated with Kelvin–Voigt element i. Using this function, the constitutive equation is written as [22,23]:

$$\varepsilon(t) = J(t)\sigma_0 + \int_0^t J(t-s)\frac{d\sigma(t)}{dt}ds \quad (4)$$

where s is a time variable, σ_0 is the stress at the time zero, and $\varepsilon(t)$ is the strain function.

Alternatively, the viscoelastic behavior can be described using the relaxation function, and the constitutive equation is written as [22,23]:

$$\sigma(t) = \int_{-\infty}^{t} G(t-s)\frac{d\varepsilon(t)}{dt}ds \quad (5)$$

where $G(t)$ is the stress relaxation function. $G(t)$ is related to the creep compliance function, $J(t)$, in the Laplace domain by the following relation [22,23]:

$$G(s)J(s) = \frac{1}{s^2} \quad (6)$$

The prony series representation of the stress relaxation is

$$G(t) = G_\infty + \sum_{i=1}^{5} G_i \exp\left(\frac{-t}{\tau_i}\right) \quad (7)$$

The linear creep compliance was modeled by fitting the data to the Prony series in Eq. (3). To evaluate the constants, linear creep compliances obtained at 5, 10, 15, and 20 MPa in the dry condition were averaged to yield one creep compliance curve. The retardation time was selected on a trial and error basis. Thereafter the creep compliance was fitted to Prony series using a non-linear least-square subroutine in Matlab 2006b. The calculated Prony series parameters are listed in Table 2. The creep compliance described the Kelvin–Voigt model is plotted in Fig. 8 along with experimentally measured curve. The precision of the fit can be seen. The Kelvin–Voigt model was also used for modeling the linear creep response in DMC and 1.1 M LiPF6 in EC/DMC, and the results are presented in Table 2 and Fig. 8.

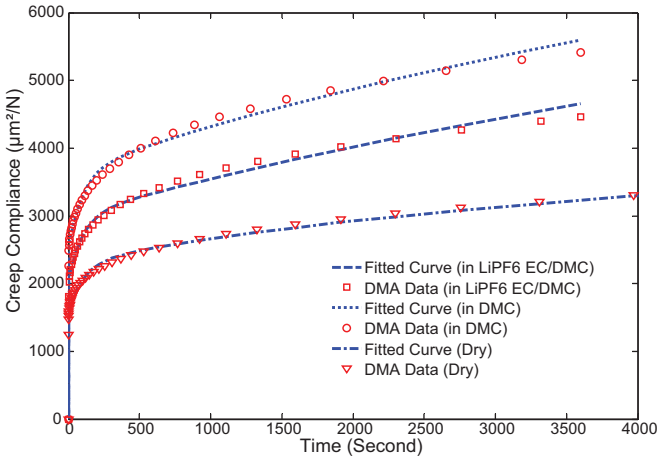

Fig. 8. Experimental creep compliances along with the fitted curves for the separator in the dry condition, DMC, and 1.1 M LiPF6 in EC/DMC.

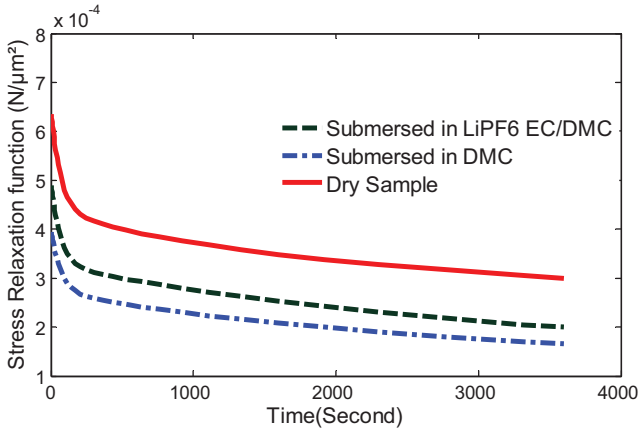

Fig. 9. Comparison of the stress relaxation functions obtained by Laplace transformation of creep compliance functions for the separator in the dry condition, DMC, and 1.1 M LiPF6 in EC/DMC.

As shown, the instantaneous creep compliances ($t = 0$) at the two wet conditions were significantly higher, which is in agreement with the results of the tensile test. Furthermore, the slopes of the creep compliance curves for the wet condition were larger and the difference between the two sets of condition increased with time. The creep tendency appears to increase in the following order: dry < 1.1 M LiPF6 in EC/DMC < DMC.

The parameters in the stress relaxation function expressed in Prony series (Eq. (7)) were obtained by Laplace transformation. The results are presented in Table 3. Fig. 9 compares the computed stress relaxation functions for the separator in the dry condition and when being submersed in DMC and in LiPF6 EC/DMC.

Table 2
Prony series parameters for the creep compliance function.

Creep constant ($m^2\ N^{-1}$)	Dry	In DMC	In 1.1 M LiPF6 EC/DMC	Retardation time (s)	
J_0	3.61×10^{-11}	3.45×10^{-12}	4.46×10^{-11}	–	–
J_1	1.52×10^{-9}	2.51×10^{-9}	1.98×10^{-9}	τ_1	0.1
J_2	7.10×10^{-10}	1.11×10^{-9}	9.69×10^{-10}	τ_2	100
J_3	2.79×10^{-10}	2.3×10^{-10}	8.78×10^{-11}	τ_3	1000
J_4	2.30×10^{-9}	5.8×10^{-9}	5.21×10^{-9}	τ_4	10,000
J_5	1.48×10^{-12}	7.14×10^{-11}	7.63×10^{-12}	τ_5	100,000

Table 3
Prony series parameters for the stress relaxation function.

Dry		In DMC		In 1.1 M LiPF6 EC/DMC	
Stress relaxation constant ($N\,m^{-2}$)	Relaxation time (s)	Stress relaxation constant ($N\,m^{-2}$)	Relaxation time (s)	Stress relaxation constant ($N\,m^{-2}$)	Relaxation time (s)
$G_0 = 2.1 \times 10^8$	–	$G_0 = 1.04 \times 10^8$	–	$G_0 = 1.23 \times 10^8$	–
$G_1 = 2.71 \times 10^{10}$	$\tau_1 = 0.0023$	$G_1 = 2.91 \times 10^{11}$	$\tau_1 = 0.00014$	$G_1 = 2.26 \times 10^{10}$	$\tau_1 = 0.0021$
$G_2 = 2.07 \times 10^8$	$\tau_2 = 68.24$	$G_2 = 1.26 \times 10^8$	$\tau_2 = 68.7853$	$G_2 = 1.69 \times 10^8$	$\tau_2 = 66.33$
$G_3 = 5.32 \times 10^7$	$\tau_3 = 884.39$	$G_3 = 2.11 \times 10^7$	$\tau_3 = 932.33$	$G_3 = 1.22 \times 10^7$	$\tau_3 = 968.07$
$G_4 = 1.75 \times 10^8$	$\tau_4 = 5322.9$	$G_4 = 1.48 \times 10^8$	$\tau_4 = 4064.3$	$G_4 = 1.92 \times 10^8$	$\tau_4 = 3860.3$
$G_5 = 5.69 \times 10^4$	$\tau_5 = 99{,}971$	$G_5 = 1.46 \times 10^5$	$\tau_5 = 99{,}850$	$G_5 = 2.81 \times 10^5$	$\tau_5 = 99{,}756$

Table 4
Average storage moduli and loss moduli.

Test condition	Storage modulus (MPa)			Loss modulus (MPa)		
	0.1 Hz	1 Hz	10 Hz	0.1 Hz	1 Hz	10 Hz
Dry, MD	924	1047	1192	116	120	136
Dry, TD	411	452	502	45	48	56
Submersed in DMC, MD (ratio to dry)	433 (0.469)	473 (0.452)	523 (0.439)	41 (0.353)	42 (0.350)	66 (0.485)
Submersed in DMC, TD (ratio to dry)	237 (0.577)	252 (0.558)	271 (0.540)	26.5 (0.589)	24.5 (0.510)	28.5 (0.509)

According to this prediction, the stress relaxation will occur rapidly in the first 200 s and then continue at a slower pace.

3.3. Frequency sweep

The viscoelastic property of the separator was studied through a frequency sweep experiment where the sample was subjected to an oscillation of low amplitude over a wide range of frequencies. This measurement provides information about the molecular and intermolecular deformation mechanisms in the material during the frequency sweep [24].

In these experiments, a preload equal to 0.1 N (0.66 MPa) was applied to the sample prior to subjecting it to oscillations, with an amplitude of 150 μm, along a log based frequency sweep, from 0.1 Hz to 10 Hz, with a total of 19 distinct frequencies. The frequency sweep tests were carried out for samples in both dry and wet condition (DMC) in both the MD and the TD.

Fig. 10a compares the results in the dry and wet condition (DMC) in MD. Within the frequency range of 0.1–10 Hz, the storage modulus E' and loss modulus E'' increased steadily with the frequency. Their values at 0.1 Hz, 1 Hz, and 10 Hz are provided in Table 4. The spectrum of damping factor tan δ exhibits no distinguishable peak, indicating there is no visible change in the deformation mechanism within this range. In DMC, both E' and E'' of the samples were significantly lower than those in the dry condition. For E', the ratio of wet to dry was in the range of 0.44–0.47 in MD and 0.54–0.57 in TD. In DMC, the damping factor was lower at low frequencies but became higher at the high frequency end when compared to that in the dry condition. The results in TD showed a similar trend (Fig. 10b).

Table 5 compares the Young's modulus obtained from tensile test and the complex modulus determined from the viscoelastic measurement. The complex modulus E^* is defined by:

$$E^* = \sqrt{(E')^2 + (E'')^2} \tag{8}$$

Table 5
Comparison of the Young's moduli and the complex moduli at 0.1 Hz.

	Young's modulus (MPa)	Complex modulus (MPa)
Dry, MD	843 ± 20	931 ± 42
Dry, TD	430 ± 23	413 ± 47
Submersed in DMC, MD (ratio to dry)	409 ± 28 (0.485)	434 ± 38 (0.466)
Submersed in DMC, TD (ratio to dry)	377 ± 10 (0.877)	238 ± 40 (0.576)

Once again, the results showed that the moduli tested in DMC were significantly lower than those tested in the dry condition. The ratio of wet to dry for E^* is 0.466 in MD, which is close to the ratio for Young's modulus of 0.485.

It should be noted that the results of this study are consistent with previous observations [20] that, when being tested in a dry condition, the difference between separator materials as received and after being soaked in electrolyte solutions is small. In this study, to examine the effect of precondition, a number of MD samples that had been submersed in two types of solutions were tested after drying. The measured stress–strain curves were similar to those tested in as received condition. However, contrary to current common

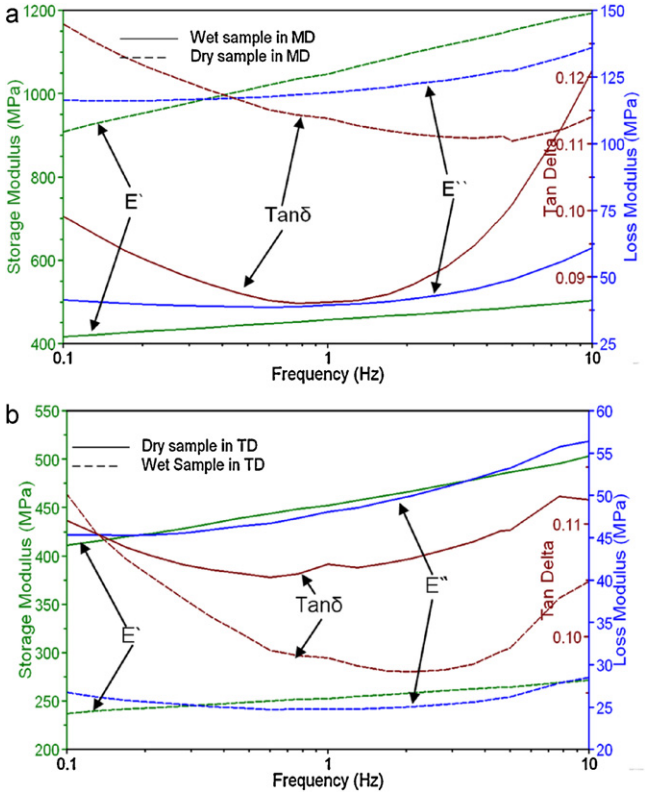

Fig. 10. Comparison of the results of frequency sweep/isothermal temperature tests (a) in the dry condition and (b) in DMC.

believes, this study revealed that the electrolyte solutions indeed have a significant effect on the mechanical property of the separator. To demonstrate this, the measurements must be performed while the sample is submersed in solutions. The study is ongoing to uncover the possible mechanisms governing this behavior.

4. Conclusion

Tensile stress–strain, creep, and viscoelastic characterizations were performed on a polypropylene separator designed for lithium-ion batteries. The measurements were carried out in both dry and wet conditions. In the wet condition, the samples were submerged into either a DMC solvent or a solution of 1.1 M LiPF6 in EC/DMC. Results revealed that the mechanical responses of the samples in solutions were significantly softer relative to the dry tested samples. The wet to dry ratio for the Young's modulus was 0.485 in the MD and 0.877 in the TD, and for the yield strength was 0.747 in the TD when measured in DMC. A series of dry and wet creep and creep recovery tests were also carried out for both the MD and TD. The range for a linear viscoelastic response is at least up to 20 MPa and 12 MPa in MD in dry and in solutions, respectively. The frequency sweep tests in the range of 0.1–10 Hz showed a reduction in the complex modulus and damping in samples tested in submersed condition. The behavior in 1.1 M LiPF6 in EC/DMC was similar to that in DMC but appear to be stiffer. All results indicate that the mechanical properties measured at the dry condition are not sufficient to represent the material's in situ behavior.

Acknowledgments

The authors would like to thank Jixing Wang of Jilin University, Hamid Kia and Mark Verbrugge of General Motors for their contributions and valuable discussions to this investigation. This project is supported by General Motors Company under a research contract ND4306101-LT442 and by NSF CMMI-1030821. A. Sheidaei would like to acknowledge the generous support from the Zonta International Foundation for the Amelia Earhart Fellowship.

References

[1] P. Arora, Z.M. Zhang, Chemical Reviews 104 (2004) 4419–4462.
[2] S.S. Zhang, Journal of Power Sources 164 (2007) 351–364.
[3] R. Baldwin, NASA/TM-2009-215590, 2009.
[4] X. Huang, Journal of Solid State Electrochemistry 15 (2011) 649–662.
[5] E.P. Roth, D.H. Doughty, D.L. Pile, Journal of Power Sources 174 (2007) 579–583.
[6] S. Santhanagopalan, P. Ramadass, J.Z. Zhang, Journal of Power Sources 194 (2009) 550–557.
[7] E. Darcy, Journal of Power Sources 174 (2007) 575–578.
[8] R.M. Spotnitz, J. Weaver, G. Yeduvaka, D.H. Doughty, E.P. Roth, Journal of Power Sources 163 (2007) 1080–1086.
[9] W. Böhnstedt, Journal of Power Sources 67 (1997) 299–305.
[10] M.D. Farrington, Journal of Power Sources 80 (1999) 278–285.
[11] M.D. Farrington, Journal of Power Sources 96 (2001) 260–265.
[12] X. Xiao, W. Wu, X. Huang, Journal of Power Sources 195 (2010) 7649–7660.
[13] D. Shi, X. Xiao, X. Huang, H. Kia, Journal of Power Sources, 2011, doi:10.1016/j.jpowsour.2011.05.026.
[14] W. Wu, X. Xiao, D. Shi, IMECE2010-37870, ASME Congress, Vancouver, Nov. 2010.
[15] G. Venugopal, J. Moore, J. Howard, S. Pendalwar, Journal of Power Sources 77 (1999) 34–41.
[16] C. Zhenyu, Doctoral thesis, Zhejiang university, 2008 (in Chinese).
[17] C. Wen-yu, Master thesis, Harbin Institute of Technology, 2006 (in Chinese).
[18] Y. Ding, W. Di, Y. Jiang, F. Xu, Z. Long, F. Ren, P. Zhang, Ionics 15 (2009) 731–734.
[19] A.S. Gozdz, J.M. Tarascon, C.N. Schmutz, P.C. Warren, O.S. Gebizlioglu, F. Shokoohi, Proceedings of the 10th Annual Battery Conference on Applications and Advances, Long Beach, CA, USA, Jan, 1995, pp. 301–306.
[20] C.T. Love, Journal of Power Sources 196 (2011) 2012–2905.
[21] TA Instruments, Dynamic Mechanical Analyser, Operator's Manual, New Castle, 2002.
[22] I.M. Ward, J. Sweeney, An Introduction to the Mechanical Properties of Solid Polymers, John Wiley & Sons Ltd, West Sussex, England, 2004.
[23] A.S. Wineman, K.R. Rajagopal, Mechanical Response of Polymers: An Introduction, Cambridge University, 2000.
[24] A. Martin, P. Bustamante, A.H.C. Chun, Physical Pharmacy: Physical Chemical Principles in the Pharmaceutical Sciences, Lea & Febiger, Philadelphia, 1993, pp. 135–137.